

Magnetocrystalline anisotropy, Dzyaloshinskii-Moriya interaction, and orbital moment anisotropy in W/Co/Pt trilayers

Zhendong Chi,¹ Yong-Chang Lau,^{1,2} Vanessa Li Zhang,³ Goro Shibata,¹ Shoya Sakamoto,¹ Yosuke Nonaka,¹ Keisuke Ikeda,¹ Yuxuan Wan,¹ Masahiro Suzuki,¹ Masako Suzuki-Sakamaki,⁴ Kenta Amemiya,⁴ Naomi Kawamura,⁵ Masaichiro Mizumaki,⁵ Motohiro Suzuki,⁵ Hyunsoo Yang,⁶ Masamitsu Hayashi,^{1,2} and Atsushi Fujimori^{1,7}

¹*Department of Physics, The University of Tokyo, Bunkyo-ku, Tokyo 113-0033, Japan*

²*National Institute for Materials Science, Tsukuba, Ibaraki 305-0047, Japan*

³*School of Physics and Technology, Wuhan University, Wuhan 430072, China*

⁴*Institute of Materials Structure Science, High Energy Accelerator Research Organization, Tsukuba, Ibaraki 305-0801, Japan*

⁵*Japan Synchrotron Radiation Research Institute (JASRI), Sayo 679-5198, Japan*

⁶*Department of Electrical and Computer Engineering,*

National University of Singapore, Singapore 117576, Singapore

⁷*Department of Applied Physics, Waseda University, Shinjuku-ku, Tokyo 169-8555, Japan*

(Dated: November 13, 2021)

We have studied the Co layer thickness dependences of magnetocrystalline anisotropy (MCA), Dzyaloshinskii-Moriya interaction (DMI), and orbital moment anisotropy (OMA) in W/Co/Pt trilayers. We find the MCA favors magnetization along the film normal and monotonically increases with decreasing effective magnetic layer thickness (t_{eff}). The magnitude of the Dzyaloshinskii-Moriya exchange constant ($|D|$) increases with decreasing t_{eff} until $t_{\text{eff}} \sim 1$ nm, below which $|D|$ decreases. MCA and $|D|$ scale with $1/t_{\text{eff}}$ for t_{eff} larger than ~ 1.0 nm, indicating an interfacial origin. To clarify the cause of the t_{eff} dependences of MCA and DMI, the OMA of Co in W/Co/Pt trilayers is studied using x-ray magnetic circular dichroism (XMCD). We find non-zero OMA when t_{eff} is smaller than ~ 0.8 nm. The OMA increases with decreasing t_{eff} at a rate that is larger than what is expected from the MCA and Bruno's formula, indicating that other factors contribute to the MCA at small t_{eff} to break the $1/t_{\text{eff}}$ scaling. The t_{eff} dependence of the OMA also suggests that $|D|$ at t_{eff} smaller than ~ 1 nm is independent of the OMA at the interface. We consider the growth of Co on W results in a strain that reduces the interfacial MCA and DMI at small t_{eff} , indicating the importance of lattice structure to control their properties.

I. INTRODUCTION

Ultrathin film heterostructures that consist of a ferromagnetic metal (FM) layer and a non-magnetic heavy metal (HM) layer are attracting great interest as phenomena that originate from the strong spin-orbit coupling of bulk and interface have been successively discovered. Efficient current-induced magnetization reversal [1] and fast motion of magnetic domain walls [2] in heterostructures with perpendicular magnetic anisotropy (PMA) in the FM layer have been observed and attributed to spin-orbit coupling-induced effects such as the spin Hall effect [3–6], the Rashba-Edelstein effect [7, 8], and the Dzyaloshinskii-Moriya interaction (DMI) [9, 10]. To stabilize chiral Néel domain walls [11–13] and skyrmions [14, 15], which are essential for potential racetrack memory applications based on FM/HM heterostructures [16–18], strong DMI is necessary [19–21]. Solid understanding on these interfacial phenomena is essential to develop systems with PMA and strong DMI.

The microscopic origins of PMA and interfacial DMI have been discussed in relation to the orbital moment anisotropy (OMA) [22, 23] and the magnetic dipole moment in the FM layer [24, 25]. Theoretically, OMA should exist both in the FM and HM elements [26]. It is thus of high importance to identify the role the OMA (of FM and HM) plays in PMA and DMI.

Here, we study the correlation between magnetocrystal-

line anisotropy (MCA), DMI and OMA in W/Co/Pt trilayers. The Co layer thickness dependences of MCA and DMI in W/Co/Pt trilayers are studied using vibrating sample magnetometer (VSM) and Brillouin light scattering spectroscopy (BLS), respectively. The Co layer thickness dependences of the spin and orbital magnetic moments of Co in W/Co/Pt trilayers and the proximity-induced magnetization (PIM) in W and Pt in W/Co and Pt/Co bilayers are studied using soft- and hard-x-ray magnetic circular dichroism (XMCD), respectively. We find the MCA, DMI, and OMA of Co show different Co layer thickness dependences in W/Co/Pt trilayers.

II. EXPERIMENT

Co thin films sandwiched by W and Pt, i.e. 3 W/ t_{Co} Co/1 Pt/1 Ru (the numbers denote the nominal thicknesses in nm, stacking order from bottom to top) were grown on 10×10 mm² thermally oxidized Si substrates by magnetron sputtering at room temperature in a base pressure better than 5×10^{-7} Pa. The top Ru layer is used to protect the trilayers from oxidation. The Co layer thickness (t_{Co}) was changed from ~ 0.6 to ~ 1.7 nm. The magnetic hysteresis loops of the samples were measured using a VSM at room temperature. The magnitude of DM exchange constant ($|D|$) was investigated by BLS [27]. X-ray absorption spectroscopy (XAS) and XMCD

measurements at the Co $L_{3,2}$ edges were performed using soft x ray at the helical undulator beamline BL-16A1 of Photon Factory, High Energy Accelerator Research Organization (KEK-PF). The spectra were measured in the total electron yield (TEY) mode, using right- ($\sigma+$) and left-hand ($\sigma-$) circularly-polarized x rays. The measurements were performed at room temperature in an ultra high vacuum (UHV) better than 5×10^{-7} Pa. The magnitude of the magnetic field was set at 5 T and the field was applied parallel to the incident x rays in all measurements. The W and Pt $L_{3,2}$ -edge XAS and XMCD measurements of 0.6 W/0.8 Co and 0.6 Pt/0.8 Co bilayers were conducted using hard x rays at BL39XU of SPring-8. The partial fluorescence yield (PFY) method and x-ray polarization switching were used in the acquisition of spectra. The measurements were performed at atmospheric pressure and at room temperature. A magnetic field of up to 2 T was applied during the measurement. In order to obtain the out-of-plane and in-plane components of the magnetic moments, magnetic field was applied to the sample along the film normal and 30° with respect to the sample surface, referred to out-of-plane and “in-plane” magnetic field hereafter.

III. RESULTS AND DISCUSSION

The magnetic properties of the trilayers are shown in Fig. 1. The t_{Co} dependence of the magnetic moment is shown in Fig. 1(a). The moment scales with t_{Co} . A linear function is fitted to the data with larger weight on the films with larger t_{Co} . The slope of the linear function is proportional to the saturation magnetization per unit volume M_s and the horizontal axis intercept represents the magnetic dead layer thickness t_D . After considering the area of samples, we find $M_s \sim 1350 \pm 50$ emu $\cdot\text{cm}^{-3}$ and $t_D \sim 0.14 \pm 0.05$ nm. The value of M_s is close to that of bulk Co [28]. t_D is typically negative when Co faces a Pt layer due to PIM [29, 30]. Positive t_D indicates that the magnetic dead layer at the W/Co interface compensates the negative t_D . We infer that the true dead layer thickness at the W/Co interface is ~ 0.2 to 0.3 nm.

The effective magnetic anisotropy energy density, K_{eff} , is obtained by taking the integrated areal difference between the easy-axis and hard-axis magnetization hysteresis loops. With the effective magnetic layer thickness defined as $t_{\text{eff}} \equiv t_{\text{Co}} - t_D$, the product of K_{eff} and t_{eff} , $K_{\text{eff}}t_{\text{eff}}$, is given by the following equation [30, 31]:

$$K_{\text{eff}}t_{\text{eff}} = K_I + (K_B - 2\pi M_s^2)t_{\text{eff}}, \quad (1)$$

where K_B and K_I represent the bulk and interfacial contributions to K_{eff} . The $2\pi M_s^2$ term represents the shape anisotropy energy density. $K_{\text{eff}}t_{\text{eff}}$ is plotted against t_{eff} in Fig. 1(b). Negative $K_{\text{eff}}t_{\text{eff}}$ corresponds to the magnetic easy axis of the samples lying along the film plane. A linear function is fitted to the data with larger weight on the films with larger t_{eff} . The slope and the y -axis intercept of the linear function represent ($K_B - 2\pi M_s^2$)

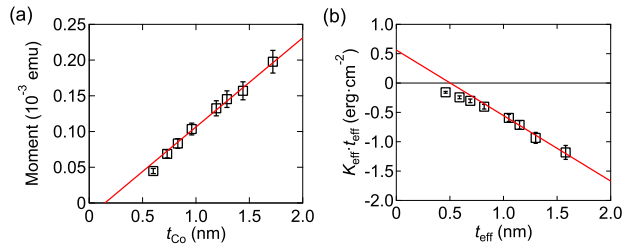


FIG. 1. (a) Magnetic moment of W/Co/Pt as a function of Co layer thickness, t_{Co} . The solid line is a linear fit to the data for $t_{\text{Co}} > 1$ nm. (b) Product of the effective magnetic anisotropy energy, K_{eff} , and effective magnetic layer thickness, t_{eff} , plotted as a function of t_{eff} . The solid line is a linear fit to the data for $t_{\text{eff}} > 1$ nm.

and K_I , respectively. From the fitting, we obtain $K_B \sim (0.8 \pm 0.7) \times 10^6$ erg $\cdot\text{cm}^{-3}$ and $K_I \sim 0.6 \pm 0.1$ erg $\cdot\text{cm}^{-2}$. M_s is obtained from the fitting shown in Fig. 1(a). K_I is smaller than that typically reported for structures which include Co/Pt interfaces [29, 30]. Note that the data show deviation from the linear fitting when t_{eff} is smaller than ~ 1.0 nm.

MCA is obtained by excluding the contribution from the shape anisotropy in K_{eff} , defined as

$$\text{MCA} \equiv K_{\text{eff}} + 2\pi M_s^2 = \frac{K_I}{t_{\text{eff}}} + K_B. \quad (2)$$

We plot the t_{eff} and $1/t_{\text{eff}}$ dependences of the MCA in Fig. 2(a) and (b). MCA increases monotonically by decreasing t_{eff} . Positive MCA favors perpendicular magnetization. According to the values obtained from the linear fitting in Fig. 1(b), contribution from K_I is considerably larger than that of K_B . We, therefore, expect the MCA to scale with $1/t_{\text{eff}}$. The calculated MCA using the parameters obtained from the fitting in Fig. 1(b) is shown by the red solid lines in Fig. 2. Although the MCA is proportional to $1/t_{\text{eff}}$ for $t_{\text{eff}} > 1$ nm, it clearly deviates from the scaling for $t_{\text{eff}} \lesssim 1$ nm.

The t_{eff} dependence of the magnitude of the

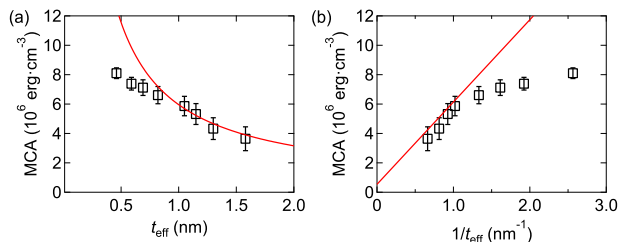


FIG. 2. t_{eff} (a) and $1/t_{\text{eff}}$ (b) dependence of magnetocrystalline anisotropy (MCA) in W/Co/Pt trilayers. The solid curves in (a) and (b) are calculated curves using Eq. (2) and the parameters obtained from the fitting shown in Fig. 1(b).

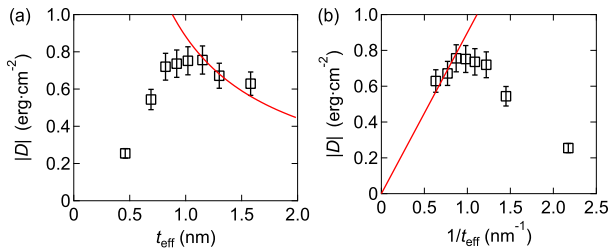


FIG. 3. t_{eff} (a) and $1/t_{\text{eff}}$ (b) dependence of the magnitude of the Dzyaloshinskii-Moriya exchange constant ($|D|$) in W/Co/Pt trilayers deduced by Brillouin light scattering spectroscopy (BLS) measurements. The solid lines in (a) and (b) show fit to the data.

Dzyaloshinskii-Moriya exchange constant ($|D|$) is plotted in Fig. 3(a). $|D|$ increases with decreasing t_{eff} until $t_{\text{eff}} \sim 1$ nm, below which it drops. A similar tendency has been observed in HM/FM systems [32, 33], which is not in accordance with the simple picture of interface-driven DMI. We plot the $1/t_{\text{eff}}$ dependence of $|D|$ in Fig. 3(b). The data are fitted using a linear function with a larger weight on the films with larger t_{eff} : the results are shown by a red solid line in Fig. 3(b). The parameters obtained from the linear fitting in Fig. 3(b) are used to calculate the $1/t_{\text{eff}}$ dependence of $|D|$ in Fig. 3(a). The calculated results are shown by a red solid line in Fig. 3(a). The experimental data deviates from the linear fitting for $t_{\text{eff}} < 1$ nm.

To identify the origin of the t_{eff} dependences of MCA and DMI in W/Co/Pt trilayers, the XAS and XMCD spectra of Co are studied. Fig. 4(a) illustrates the XAS and XMCD spectra at the Co $L_{3,2}$ edges of the W/Co/Pt trilayers measured under a magnetic field of 5 T. No obvious peak shift or spectral line-shape change is found in both the XAS and XMCD spectra, suggesting that there is no significant changes in the chemical state of Co, i.e., the oxidation of Co is negligibly small. The solid and dashed curves in Fig. 4(a) represent the spectra measured when out-of-plane and “in-plane” magnetic fields are applied, respectively. The integrated XMCD spectra, as displayed by the corresponding curves in Fig. 4(b), show clear differences under out-of-plane and “in-plane” field application. These results indicate that the magnetic moment of Co is anisotropic.

The effective spin magnetic moment (m_{eff}) of Co atom is estimated using the XMCD sum rule [34, 35]:

$$m_{\text{eff}} = m_{\text{spin}} + \frac{7}{2}m_{\text{T}} = -\frac{2 \int_{L_3} \Delta\mu d\nu - 4 \int_{L_2} \Delta\mu d\nu}{\int_{L_{3,2}} \mu d\nu} n_h, \quad (3)$$

where $\Delta\mu$ and μ are the difference and sum of the XAS spectra obtained using right- and left-handed circularly polarized light, m_{spin} is the spin magnetic moment of

Co atom, m_{T} is the magnetic dipole, n_h is the number of holes in the d band of the magnetic atom. Here, we present magnetic moments in units of Bohr magneton per hole. The out-of-plane and in-plane components of the magnetic moments are obtained from the integrated XAS/XMCD spectra measured under the out-of-plane and “in-plane” magnetic field, respectively. m_{spin} is considered to be isotropic, but m_{T} possesses an angular dependence: $m_{\text{T}} = -\frac{1}{2}m_{\text{T}_0}(1 - 3\sin^2\theta)$ [36, 37]. Here, m_{T_0} represents the out-of-plane component of m_{T} and θ is the angle between the magnetization and the film plane.

The estimated values of m_{spin} and m_{T_0} are shown in Fig. 4(c) and (d) as a function of t_{eff} , respectively. m_{spin} deviates from its bulk value, shown by a horizontal dashed line, and tends to decrease with decreasing t_{eff} . Such variation of m_{spin} with magnetic layer thickness has also been observed in similar systems [29]. m_{spin} is fitted against t_{Co} using a relation: $m_{\text{spin}} = (1 - t_{\text{D}}/t_{\text{Co}})m_{\text{spin,active}}$, where $m_{\text{spin,active}}$ is the active spin magnetic moment, to estimate the t_{D} in the Co layer. From the fitting, we obtain $t_{\text{D}} \sim 0.20 \pm 0.03$ nm, which is consistent with our assumption on the true dead layer thickness at the W/Co interface. m_{T_0} , which is considerably smaller than m_{spin} , represents the anisotropic spin-density distribution and its strength characterizes the anisotropy of the charge/spin distribution of the d orbitals. The value of m_{T_0} is positive, which means that the spin density distribution is expanded in the in-plane direction and is consistent with the MCA favoring perpendicular magnetization. Although it has been reported that m_{T_0} is related to the emergence of PMA [24] and DMI [25], here its magnitude is considerably smaller than past report [25] and the accuracy is not high enough to determine whether m_{T_0} possesses any t_{eff} dependence.

The orbital magnetic moment (m_{orb}) of Co atom is estimated using the XMCD sum rule [34, 35]:

$$m_{\text{orb}} = -\frac{4 \int_{L_{3,2}} \Delta\mu d\nu}{3 \int_{L_{3,2}} \mu d\nu} n_h. \quad (4)$$

The out-of-plane component of m_{orb} , m_{orb}^{\perp} , is estimated from the XAS and XMCD spectra measured under the out-of-plane magnetic field. The in-plane component, $m_{\text{orb}}^{\parallel}$, is obtained using the spectra measured under the out-of-plane and “in-plane” fields according to the relationship,

$$m_{\text{orb}}(\theta) = m_{\text{orb}}^{\perp} \sin^2\theta + m_{\text{orb}}^{\parallel} \cos^2\theta, \quad (5)$$

with $\theta = 30^\circ$. The t_{eff} dependence of m_{orb} is plotted in Fig. 4(e). Both m_{orb}^{\perp} and $m_{\text{orb}}^{\parallel}$ decrease with decreasing t_{eff} from their bulk value. We find the decrease of $m_{\text{orb}}^{\parallel}$ with t_{eff} is stronger than that of m_{orb}^{\perp} . This difference leads to the OMA of Co which is shown by black squares in Fig. 4(e). The normalized orbital magnetic moment

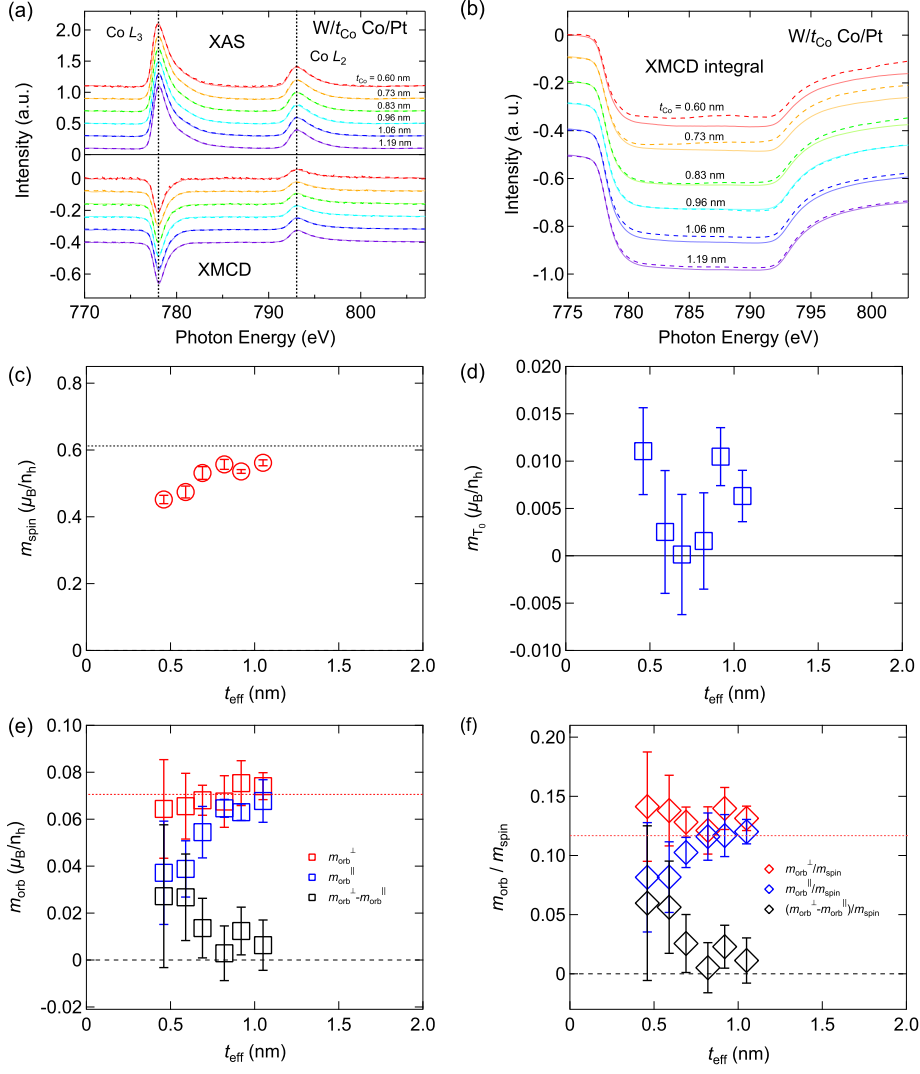


FIG. 4. XAS, XMCD spectra and magnetic moments of Co in W/Co/Pt trilayers estimated by XMCD sum rules. Spectra after background subtraction are shown. XAS, XMCD (a) and the integrated XMCD (b) spectra at the Co $L_{3,2}$ edges for samples with different Co thicknesses. The spectra obtained under the out-of-plane magnetic and “in-plane” field are plotted by solid and dashed curves, respectively. t_{eff} dependence of the spin moment (m_{spin}) (c) and the out-of-plane component of magnetic dipole (m_{T_0}) (d). t_{eff} dependence of the orbital magnetic moment (m_{orb}) and normalized orbital magnetic moment ($m_{\text{orb}}/m_{\text{spin}}$), for different magnetization directions, are shown in (e) and (f), respectively. The spin, orbital and normalized orbital moment values of bulk hcp Co [28] are shown using dashed horizontal lines in (c-e).

$m_{\text{orb}}/m_{\text{spin}}$ is plotted against t_{eff} in Fig. 4(f). The out-of-plane component, $m_{\text{orb}}^{\perp}/m_{\text{spin}}$, increases with decreasing t_{eff} whereas the in-plane component, $m_{\text{orb}}^{\parallel}/m_{\text{spin}}$, decreases. The normalized OMA of Co, illustrated by black diamonds in Fig. 4(f), increases with decreasing t_{eff} , especially for $t_{\text{eff}} \lesssim 0.8$ nm. These results indicate that the charge redistribution at the HM/Co interfaces takes place and induces OMA.

We have also performed W and Pt $L_{3,2}$ -edge XMCD measurements on W/Co and Pt/Co bilayers to study the PIM. The XAS and XMCD spectra are shown in Fig. 5. The XMCD signal is only found in the Pt/Co bilayer.

These results indicates PIM exists at the Pt/Co interface but W do not possess any induced magnetic moment.

Here, we discuss the relationship between the MCA, DMI and the OMA of Co in W/Co/Pt trilayers. The t_{eff} dependences of the three parameters are schematically illustrated in Fig. 6. MCA and $|D|$ scale with $1/t_{\text{eff}}$ for $t_{\text{eff}} \gtrsim 1$ nm, indicating an interfacial origin of the two properties. Bruno has proposed that the MCA and OMA are proportional to each other in FM monolayers [22]. Both MCA and the OMA of Co indeed increase with decreasing t_{eff} is smaller than ~ 0.8 nm. However, the OMA tends to increase more rapidly with decreasing

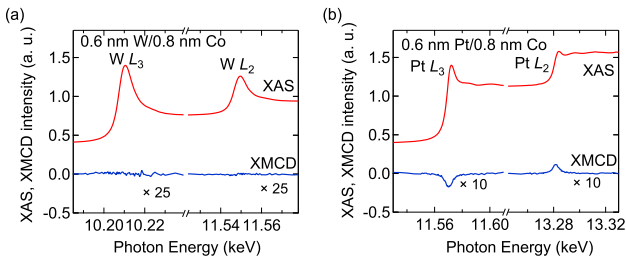


FIG. 5. XAS and XMCD spectra at the W (a) and Pt (b) $L_{3,2}$ edges in W/Co and Pt/Co bilayers. The intensity of the XMCD spectra of W (Pt) is enlarged by a factor of 25 (10).

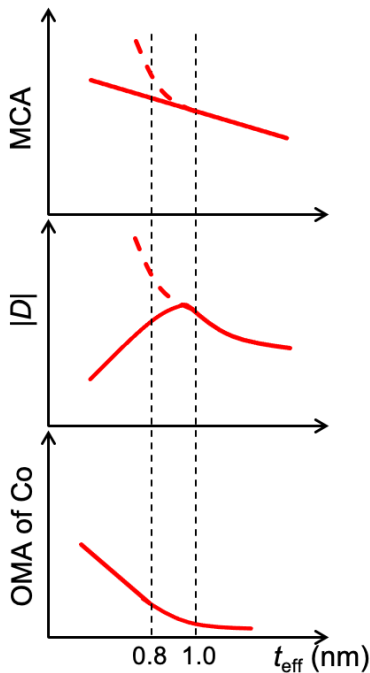


FIG. 6. Schematic illustration of the t_{eff} dependences of MCA, $|D|$, and the OMA of Co in W/Co/Pt trilayers. Dashed curves for MCA and $|D|$ indicate the $1/t_{\text{eff}}$ scaling expected for the ideal interfacial contributions.

t_{eff} than what the Bruno's law predict using the values of MCA. These results suggest additional contributions to MCA, such as strain or magnetic dipole m_{T} . Previous studies have indicated that strain and change in the film texture can weaken the MCA when the magnetic layer thickness is reduced to a few atomic planes [38, 39]. The t_{eff} dependences of MCA and $K_{\text{eff}}t_{\text{eff}}$ are in accordance with such studies. van der Laan has also shown that m_{T} affects MCA in strongly spin-orbit coupled systems, which has been associated with spin-flip virtual excitation [24]. Such relationship has been confirmed in recent experiments [40–42]. Unfortunately, the XMCD spectra of our W/Co/Pt trilayers does not have sufficient resolution to derive m_{T} accurately.

The DMI, on the other hand, approaches near zero as t_{eff} is reduced from ~ 1 nm. Interfacial DMI is due to the strong spin-orbit coupling with broken inversion symmetry. Recent studies have shown that DMI is related with m_{T} at the HM/FM interfaces [25] and the OMA of the FM atoms [23]. Comparing the results presented in Fig. 6 or in Figs. 3(a) and 4(e), we consider that such relations do not hold in this system because the t_{eff} dependence of OMA and DMI is opposite to what one expects from the scaling reported in Ref. [23]. The magnitude of m_{T} found in this system is considerably smaller than that reported in Ref. [25] and, therefore, its contribution to DMI, if any, is also likely small. We thus infer that the DMI is more sensitive to strain effect or the (111) texture of Co. Theoretical studies [43, 44] have indicated that the crystal structure at the HM/FM interface influences the strength of DMI dramatically. In the present case, strain and texture of the Co layer near the W/Co interface may significantly degrade $|D|$ for $t_{\text{eff}} \lesssim 1$ nm. With increasing Co thickness, such effects are then mitigated by the Co/Pt interface that favors the (111) texture.

IV. SUMMARY

In summary, we have studied the effective magnetic layer thickness (t_{eff}) dependences of magnetocrystalline anisotropy (MCA), Dzyaloshinskii-Moriya interaction (DMI), and orbital moment anisotropy (OMA) in W/Co/Pt trilayers. For t_{eff} larger than ~ 1 nm, MCA and DMI scale with $1/t_{\text{eff}}$, indicating an interfacial origin. Whereas MCA continues to increase with decreasing t_{eff} , DMI tends to decrease when t_{eff} is smaller than ~ 1 nm. The OMA of Co deduced from x-ray magnetic circular dichroism (XMCD) measurements is almost zero (below the detection limit) when t_{eff} is larger than ~ 0.8 nm, below which the OMA of Co increases with decreasing t_{eff} . The rate at which the OMA of Co increases with decreasing t_{eff} is larger than what is predicted from the MCA using Bruno's formula. The reduction of DMI with decreasing t_{eff} for films with $t_{\text{eff}} \lesssim 1$ nm, despite the presence of OMA, suggests that other factors contribute to the DMI in this thickness range. We infer that the strain in the Co layer induced by the W underlayer significantly weakens the DMI and, to a lesser extent, the MCA.

ACKNOWLEDGMENTS

We thank H. Shimazu for samples preparation. This work was supported by Grants-in-Aid for Scientific Research from JSPS (Grant Nos. 15H02109, 15H05702, 15K17696 and 16H03853). The XMCD experiment was performed at BL-16A of KEK-PF with the approval of the Photon Factory Program Advisory Committee (proposal Nos. 2016S2-005 and 2016G066) and at BL39XU of SPring-8 with the approval of the Japan Synchrotron Radiation Research Institute (JASRI) (proposal Nos.

2017A1048 and 2018A1058). M.H. and A.F. are adjunct members of Center for Spintronics Research Network (CSRN), the University of Tokyo, under Spintronics Research Network of Japan (Spin-RNJ). Z.C. is supported by Materials Education program for the future leaders in Research, Industry, and Technology (MERIT) and JSR Fellowship, The University of Tokyo. Y.-C.L. is

supported by JSPS International Fellowship for Research in Japan (Grant No. JP17F17064). S.S. and Y.-X.W. acknowledges financial support from Advanced Leading Graduate Course for Photon Science (ALPS). S.S. acknowledges financial support from the JSPS Research Fellowship for Young Scientists.

-
- [1] I. M. Miron, K. Garello, G. Gaudin, P. J. Zermatten, M. V. Costache, S. Auffret, S. Bandiera, B. Rodmacq, A. Schuhl, and P. Gambardella, *Nature* **476**, 189 (2011).
- [2] I. M. Miron, T. Moore, H. Szabolcs, L. D. Budaprebeanu, S. Auffret, B. Rodmacq, S. Pizzini, J. Vogel, M. Bonm, A. Schuhl, and G. Gaudin, *Nat. Mat.* **10**, 419 (2011).
- [3] M. I. Dyakonov and V. I. Perel, *Jetp Letters-Ussr* **13**, 467 (1971).
- [4] J. E. Hirsch, *Phys. Rev. Lett.* **83**, 1834 (1999).
- [5] J. Sinova, S. O. Valenzuela, J. Wunderlich, C. H. Back, and T. Jungwirth, *Rev. Mod. Phys.* **87**, 1213 (2015).
- [6] L. Liu, C.-F. Pai, Y. Li, H. W. Tseng, D. C. Ralph, and R. A. Buhrman, *Science* **336**, 555 (2011).
- [7] Y. A. Bychkov and E. I. Rashba, *Jetp Lett.* **39**, 78 (1984).
- [8] V. M. Edelstein, *Solid State Communications* **73**, 233 (1990).
- [9] I. E. Dzyaloshinskii, *JETP* **5**, 1259 (1957).
- [10] T. Moriya, *Phys. Rev.* **120**, 91 (1960).
- [11] M. Bode, M. Heide, K. von Bergmann, P. Ferriani, S. Heinze, G. Bihlmayer, A. Kubetzka, O. Pietzsch, S. Blügel, and R. Wiesendanger, *Nature* **447**, 190 (2007).
- [12] M. Heide, G. Bihlmayer, and S. Blügel, *Phys. Rev. B* **78**, 140403 (2008).
- [13] S. Emori, U. Bauer, S.-M. Ahn, E. Martinez, and G. S. D. Beach, *Nat. Mater.* **12**, 611 (2013).
- [14] B. B. S. Mühlbauer, F. Jonietz, C. Pfleiderer, A. Rosch, A. Neubauer, R. Georgii, and P. Böi, *Science* **323**, 915 (2009).
- [15] X. Z. Yu, Y. Onose, N. Kanazawa, J. H. Park, J. H. Han, Y. Matsui, N. Nagaosa, and Y. Tokura, *Nature* **465**, 901 (2010).
- [16] S. S. P. Parkin, M. Hayashi, and L. Thomas, *Science* **320**, 190 (2008).
- [17] M. Hayashi, L. Thomas, R. Moriya, C. Rettner, and S. S. P. Parkin, *Science* **320**, 209 (2008).
- [18] A. Fert, V. Cros, and J. Sampaio, *Nat. Nanotech.* **8**, 152 (2013).
- [19] A. Thiaville, S. Rohart, É. Jué, V. Cros, and A. Fert, *Europhys. Lett.* **100**, 5 (2012).
- [20] S. Tacchi, R. E. Troncoso, M. Ahlberg, G. Gubbiotti, M. Madami, J. Åkerman, and P. Landeros, *Phys. Rev. Lett.* **118**, 147201 (2017).
- [21] X. Ma, G. Yu, S. A. Razavi, S. S. Sasaki, X. Li, K. Hao, S. H. Tolbert, K. L. Wang, and X. Li, *Phys. Rev. Lett.* **119**, 027202 (2017).
- [22] P. Bruno, *Phys. Rev. B* **39**, 865 (1989).
- [23] K. Yamamoto, A.-M. Pradipto, K. Nawa, T. Akiyama, T. Ito, T. Ono, and K. Nakamura, *AIP Adv.* **7**, 056302 (2017).
- [24] G. van der Lann, *J. Phys.: Condens. Matter* **10**, 3239 (1998).
- [25] S. Kim, K. Ueda, G. Go, P.-H. Jang, K.-J. Lee, A. Belabbes, A. Manchon, M. Suzuki, Y. Kotani, T. Nakamura, K. Nakamura, T. Koyama, D. Chiba, K. Yamada, D.-H. Kim, T. Moriyama, K.-J. Kim, and T. Ono, *Nat. Commun.* **9**, 1648 (2018).
- [26] I. V. Solov'yev, P. H. Dederichs, and I. Mertig, *Phys. Rev. B* **52**, 13419 (1995).
- [27] K. Di, V. L. Zhang, H. S. Lim, S. C. Ng, M. H. Kuok, J. Yu, J. Yoon, X. Qiu, and H. Yang, *Phys. Rev. Lett.* **114**, 047201 (2015).
- [28] J. M. D. Coey, *Magnetism and magnetic materials* (Cambridge, U.K., 2010).
- [29] T. Ueno, J. Sinha, N. Inami, Y. Takeichi, S. Mitani, K. Ono, and M. Hayashi, *Sci. Rep.* **5**, 14858 (2015).
- [30] Y.-C. Lau, Z. Chi, T. Taniguchi, M. Kawaguchi, G. Shibata, N. Kawamura, M. Suzuki, S. Fukami, A. Fujimori, H. Ohno, and M. Hayashi, *Phys. Rev. Mater.* **3**, 104419 (2019).
- [31] J. Sinha, M. Hayashi, A. J. Kellock, S. Fukami, M. Yamanouchi, H. Sato, S. Ikeda, S. Mitani, S.-H. Yang, S. S. P. Parkin, and H. Ohno, *Appl. Phys. Lett.* **102**, 242405 (2013).
- [32] J. Cho, N.-H. Kim, S. Lee, J.-S. Kim, R. Lavrijsen, A. Solignac, Y. Yin, D.-S. Han, N. J. van Hoof, H. J. Swagten, B. Koopmans, and C.-Y. You, *Nat. Commun.* **6**, 7635 (2015).
- [33] M. Belmeguenai, M. S. Gabor, Y. Roussigné, T. P. Jr., R. B. Mos, A. Stashkevich, S. M. Chérif, and C. Tiusan, *Phys. Rev. B* **97**, 054425 (2018).
- [34] B. T. Thole, P. Carra, F. Sette, and G. van der Laan, *Phys. Rev. Lett.* **68**, 1943 (1992).
- [35] P. Carra, B. T. Thole, M. Altarelli, and X. Wang, *Phys. Rev. Lett.* **70**, 694 (1993).
- [36] R. Wu and A. J. Freeman, *Phys. Rev. Lett.* **73**, 1994 (1994).
- [37] J. Stöhr, *J. Magn. Magn. Mater.* **200**, 470 (1999).
- [38] M. T. Johnson, P. J. H. Bloemen, F. J. A. den Broeder, and J. J. de Vries, *Rep. Prog. Phys.* **59**, 1409 (1996).
- [39] Y.-C. Lau, P. Sheng, S. Mitani, D. Chiba, and M. Hayashi, *Appl. Phys. Lett.* **110**, 022405 (2017).
- [40] S. Miwa, M. Suzuki, M. Tsujikawa, K. Matsuda, T. Nozaki, K. Tanaka, T. Tsukahara, K. Nawaoka, M. Goto, Y. Kotani, T. Ohkubo, F. Bonell, E. Tamura, K. Hono, T. Nakamura, M. Shirai, S. Yuasa, and Y. Suzuki, *Nat. Commun.* **8**, 15848 (2017).
- [41] K. Ikeda, T. Seki, G. Shibata, T. Kadono, K. Ishigami, Y. Takahashi, M. Horio, S. Sakamoto, Y. Nonaka, M. Sakamaki, K. Amemiya, N. Kawamura, M. Suzuki, K. Takanashi, and A. Fujimori, *Appl. Phys. Lett.* **111**, 142402 (2017).
- [42] G. Shibata, M. Kitamura, M. Minohara, K. Yoshimatsu, T. Kadono, K. Ishigami, T. Harano, Y. Takahashi,

- S. Sakamoto, Y. Nonaka, K. Ikeda, Z. Chi, M. Furuse, S. Fuchino, M. Okano, J. i. Fujimori, A. Uchida, K. Watanabe, H. Fujihira, S. Fujihira, A. Tanaka, H. Kumigashira, T. Koide, and A. Fujimori, *npj Quan. Mat.* **3**, 3 (2018).
- [43] H. Yang, A. Thiaville, S. Rohart, A. Fert, and M. Chshiev, *Phys. Rev. Lett.* **115**, 267210 (2015).
- [44] A. Hrabec, N. A. Porter, A. Wells, M. J. Benitez, G. Burnell, S. McVitie, D. McGrouther, T. A. Moore, and C. H. Marrows, *Phys. Rev. B* **90**, 020402 (2014).